Enthalpy/Entropy Compensation: Influence of DNA Flanking Sequence on the Binding of 7-Amino Actinomycin D to Its Primary Binding Site in Short DNA Duplexes†

Xiaogang Qu,*,‡ Jinsong Ren,‡ Peter V. Riccelli,§ Albert S. Benight,§,|| and Jonathan B. Chaires⊥

Key Laboratory of Rare Earth Chemistry and Physics, Changchun Institute of Applied Chemistry, Chinese Academy of Sciences, Changchun, Jilin 130022, China, Department of Chemistry, University of Illinois, 845 West Taylor Street, Room 4500, Chicago, Illinois 60607, and Department of Biochemistry, School of Medicine, University of Mississippi Medical Center, 2500 North State Street, Jackson, Mississippi 39216-4505

Received May 13, 2003; Revised Manuscript Received August 14, 2003

ABSTRACT: The effect of the context of the flanking sequence on ligand binding to DNA oligonucleotides that contain consensus binding sites was investigated for the binding of the intercalator 7-amino actinomycin D. Seven self-complementary DNA oligomers each containing a centrally located primary binding site, 5′-A-G-C-T-3′, flanked on either side by the sequences $(AT)_n$ or $(AA)_n$ (with $n = 2, 3, 4$) and $AA(AT)_2$, were studied. For different flanking sequences, $(AA)_n$-series or $(AT)_n$-series, differential fluorescence enhancements of the ligand due to binding were observed. Thermodynamic studies indicated that the flanking sequences not only affected DNA stability and secondary structure but also modulated ligand binding to the primary binding site. The magnitude of the ligand binding affinity to the primary site was inversely related to the sequence dependent stability. The enthalpy of ligand binding was directly measured by isothermal titration calorimetry, and this made it possible to parse the binding free energy into its energetic and entropic terms. Our results reveal a pronounced enthalpy−entropy compensation for 7-amino actinomycin D binding to this family of oligonucleotides and suggest that the DNA sequences flanking the primary binding site can strongly influence ligand recognition of specific sites on target DNA molecules.

There are several principal components that combine to stabilize DNA−drug interactions, which include the following: drug structure (*1*−*4*) (size and stereochemistry); solution conditions (*5*−*9*) (ionic strength, pH, and temperature); and DNA sequence dependent conformation and deformability (*10*−*14*). Ligands with high binding affinity and strong selectivity have potentially useful genomic based therapeutic and diagnostic applications. Thus, understanding how both the drug and the DNA contribute to the overall stabilizing (and destabilizing) forces in complex formation is fundamental to the full characterization of drug interactions. Crystallography, NMR, and footprinting studies (*15*−*18*) have revealed that drugs have preferred binding sequences, referred to as primary binding sites. Footprinting methods have provided an especially elegant and relatively simple means for identifying longer DNA sequences that are bound specifically by drug molecules (*17*, *18*). Interestingly, a frequent observation encountered in footprinting experiments is the enhanced cleavage rates of DNase I at sequences immediately flanking primary drug binding sites (*18*). This suggests that drug molecules bound to the primary binding sites can influence DNA reactivity (DNase I attack) at adjacent flanking sequences. Such effects are usually referred to as context effects (*18*). Except for only a few studies, the context effects on binding has not been well-characterized (*19*−*21*). In this report, the binding of 7-amino actinomycin D (7-amino ACTD, a fluorescent derivative of the antitumor agent, actinomycin D) to a set of seven DNA oligomer duplexes was investigated. The DNA molecules range in length from 12 to 20 base pairs and contain the same central primary binding site (AGCT) flanked by A·T (T·A) sequences in different contexts. This set of molecules was used to investigate (in a well-defined experimental system) the effects of different flanking sequences surrounding a primary binding site on the overall binding interaction of the ligand with DNA.

DNA molecules used in this study are comprised of two 12-mers, three 14-mers, and two 20-mers. Their sequences and the structures of actinomycin D and 7-amino actinomycin D are shown in Figure 1. The set of seven molecules are formed from self-complementary strands and contain the common central four base sequence 5′-A-G-C-T-3′ flanked on both sides, by either $(AT)_n$ or $(AA)_n$, $n = 2, 3, 4$, or $AA(AT)_2$. Therefore, for the $(AT)_n$ and $(AA)_n$ series, the number of A·T (T·A) base pairs is the same, the only difference is the order of the A·T and T·A base pairs flanking the central binding site sequence (AGCT). With this design,

† Supported by Grant CA35635 (J.B.C.) from the National Cancer Institute, distinguished young scholar fund from NSFC, and hundred people program from CAS.

* Corresponding author. Tel.: 86-0431-526-2656. Fax: 86-0431-526-2656. E-mail: xqu@ciac.jl.cn.

‡ Chinese Academy of Sciences.

§ University of Illinois.

|| Present address: Department of Chemistry, Portland State University, P.O. Box 751, Portland, OR 97207.

⊥ University of Mississippi Medical Center.

10.1021/bi0347813 CCC: $25.00
Published on Web 09/23/2003

A

DNA Sequence	Abbreviation
12mers	
5'-A-A-A-A-***A-G-C-T***-T-T-T-T-3'	$(AA)_2$
3'-T-T-T-T-***T-C-G-A***-A-A-A-A-5'	
5'-A-T-A-T-***A-G-C-T***-A-T-A-T-3'	$(AT)_2$
3'-T-A-T-A-***T-C-G-A***-T-A-T-A-5'	
16mers	
5'-A-A-A-A-A-A-***A-G-C-T***-T-T-T-T-T-T-3'	$(AA)_3$
3'-T-T-T-T-T-T-***T-C-G-A***-A-A-A-A-A-A-5'	
5'-A-T-A-T-A-T-***A-G-C-T***-A-T-A-T-A-T-3'	$(AT)_3$
3'-T-A-T-A-T-A-***T-C-G-A***-T-A-T-A-T-A-5'	
5'-A-A-A-T-A-T-***A-G-C-T***-A-T-A-T-T-T-3'	$(AA)(AT)_2$
3'-T-T-T-A-T-A-***T-C-G-A***-T-A-T-A-A-A-5'	
20mers	
5'-A-A-A-A-A-A-A-A-***A-G-C-T***-T-T-T-T-T-T-T-T-3'	$(AA)_4$
3'-T-T-T-T-T-T-T-T-***T-C-G-A***-A-A-A-A-A-A-A-A-5'	
5'-A-T-A-T-A-T-A-T-***A-G-C-T***-A-T-A-T-A-T-A-T-3'	$(AT)_4$
3'-T-A-T-A-T-A-T-A-***T-C-G-A***-T-A-T-A-T-A-T-A-5'	

B

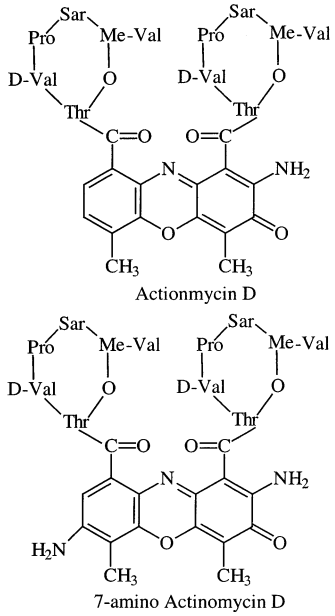

FIGURE 1: Panel A: set of seven DNA oligomer duplexes studied. Bold italicized letters denote the primary binding site for 7-amino actinomycin D. The different 5′-flanking sequences are denoted on the right. Panel B: chemical structures of actinomycin D and 7-amino actinomycin D.

any differences in the nearest neighbor contributions to DNA stability and/or subtle structural/conformational deviations between any two duplexes of the same length should be attributable to differences in only flanking sequence contexts. Thermodynamic studies in this work demonstrate that 7-amino ACTD, which binds to the DNA central core sequence (*22*), 5′-A-G-C-T-3′, is capable of distinguishing between two DNA sequence isomers, the $(AT)_nAGCT(TA)_n$ and $(AA)_nAGCT(TT)_n$ sequences. Furthermore, the DNA molecules studied here show an inverse relationship between the binding affinity to 7-amino ACTD and the flanking sequence dependent properties of the DNA. Enthalpy/entropy compensation accounts for these observations for the binding of 7-amino ACTD to the seven DNA molecules.

MATERIALS AND METHODS

7-Amino ACTD (Mol. wt. 1270.45) was purchased from Molecular Probes (Eugene, OR). Ligand concentrations were determined spectroscopically using a molar extinction coefficient of 23 600 M^{-1} cm^{-1} at 528 nm (*21*). The DNA oligomers were synthetically prepared and characterized for purity by polyacrylamide gel electrophoresis according to previously established protocols (*23*, *24*). These oligomers were self-complementary, and their duplexes were prepared by heating the oligomers to 90 °C for 3 min, slowly cooling to room temperature, and then equilibrating for 48 h at 4 °C before use. Concentrations of these oligomers were determined by measuring the absorbance at 260 nm after melting. Extinction coefficients were estimated by the nearest-neighbor method using mono- and dinucleotide values tabulated in ref *25*. All experiments were carried out in aqueous BPES buffer (6 mM Na_2HPO_4, 2 mM NaH_2PO_4, 1 mM Na_2EDTA, 0.185 M NaCl, pH = 7.0) unless noted otherwise.

Absorbance measurements and melting experiments were made on a Varian Cary 3E UV−vis spectrophotometer (Palo Alto, CA), equipped with a Peltier temperature control accessory, interfaced to a Gateway 386 PC for data collection and analysis (*26*). All melting studies were carried out using 1 cm path length cells with Teflon stoppers. Absorbance changes at 260 nm versus temperature were collected at a heating rate of 0.5 °C min^{-1}, over the temperature range of 10−100 °C. Circular dichroism spectra were measured at 20 °C on a Jasco J500A spectropolarimeter as previously described (*27*). DNA strand concentrations were about 3.0 μM (strand) in BPES buffer.

Fluorescence titration experiments were carried out at 20 °C on an I.S.S. Greg200 spectrofluorometer employing a Model ATF 105 automated titrating differential/ratio spectrofluometer (AVIV, Lakewood, NJ), equipped with a NESLAB temperature control accessory. Lifetime measurements were also recorded on the I.S.S. K2 multifrequency cross-correlation phase and modulation fluorometer, using a xenon arc lamp as a light source and a glycogen scatterer (0.5 mg/mL aqueous solution) as reference (*4*). An excitation wavelength of 505 nm was used. Fluorescence emission was monitored by collecting all emitted light passing through a 515-nm cutoff filter to eliminate scattering radiation from the light source. Lifetime determinations were performed at 15 frequencies in a 1−200 MHz range. Data were collected until the standard deviation for each measurement had a phase and modulation no greater than 0.20 and 0.004, respectively.

Isothermal Titration Calorimetry (ITC). ITC experiments were carried out with an isothermal microtitration calorimeter (ITC Model 4200, Calorimetric Sciences Corp. Provo, UT). Titrations were carried out at 20 °C (±0.01). Standard protocols for sample preparation and injection were followed as previously described (*28*). The DNA concentration in ITC experiments was 100 μM (strands) = 50 μM (duplex). Serial

injections (3 μL) of a stock 7-amino ACTD solution (0.3 mM) were added at 300-s time intervals to a DNA reaction solution. A separate ITC experiment was performed for the seven DNA molecules in Figure 1. Control experiments were carried out to calculate the heats of dilution for ligand titrated into buffer. The net enthalpy for each ligand−DNA interaction was determined by subtracting the heats of dilution for the buffer from the ligand−DNA titration curves. At least three titration experiments were performed for each DNA molecule in the set. The experimental error of the heat signal was not more than 10%. Therefore, the binding enthalpy for the ligand was determined by using the model-free ITC protocol to obtain multiple estimates of $\Delta H°$ and avoid any possible fitting bias (*29*). This procedure allows the acquisition of an accurate binding enthalpy but is not appropriate to estimate the binding constant. The binding constant was determined by the fluorescence titration method.

Fluorescence Enhancement Experiments. Primary fluorescence excitation and emission spectra of 7-amino ACTD alone and with the $(AA)_n$ or $(AT)_n$ series (the ratio, r = **[**ligand**]**/[DNA] = 1:100) were recorded at λ_{em} = 650 nm or at λ_{ex} = 505 nm in BPES buffer at 20 °C.

Determination of Binding Constants. A fluorescence based titration assay was utilized to evaluate the binding constants for the interaction of 7-amino ACTD with each of the seven DNA duplex molecules. Binding isotherms were obtained by measuring the fluorescence of a fixed concentration of $(AA)_n$- or $(AT)_n$-series DNA with varying concentrations of 7-amino ACTD.

As shown in Figure 1, and described above, each DNA in the set contains a single preferential binding site for 7-amino ACTD (*22*). This eliminates the need to apply neighbor exclusion and/or cooperative binding terms in the analysis of the binding curves (*30*, *31*). Alternatively, the uncoupled saturation model was used to verify a 1:1 (ligand/DNA) binding stoichiometry. Binding curves were analyzed by an iterative nonlinear least-squares fitting method (FitAll, Toronto) using the following expression:

$$r = KnC_f/(1 + KC_f)$$

Where r is the ratio of the concentration of bound ligand to the total duplex concentration, n is their binding stoichiometry, and C_f is the concentration of free ligand. Errors in the binding parameters resulting from the fitting procedure were carefully evaluated by Monte Carlo analysis (*27*).

RESULTS AND DISCUSSION

7-Amino ACTD and its derivatives are DNA-binding antitumor agents that act in vivo by inhibiting DNA dependent RNA polymerase activities (*32*, *33*). Structural studies and footprinting results have shown that the planar chromophore portions of 7-amino ACTD intercalate into 5′GpC3′ sequences via the minor groove. Additional complex stabilization is accomplished through the two cyclic pentapeptide lactone substituents anchoring along both sides of the minor groove covering a span of four base pairs, which comprise the total primary binding site (*21*, *22*). The relatively larger primary binding sites that result from interactions beyond the GpC regions makes 7-amino ACTD a good candidate to study DNA sequence context effects on ligand binding (*22*, *23*). Results of thermodynamic studies presented here demonstrate that sequences flanking the primary binding site of 7-amino ACTD strongly influence the DNA stability and modulate 7-amino ACTD binding at the site as well. Specifically, increasing the flanking sequence dependent DNA stability appears to decrease 7-amino ACTD binding affinity. Such effects may originate from the enthalpy/entropy compensation inferred from calorimetry experiments of 7-amino ACTD/DNA interactions.

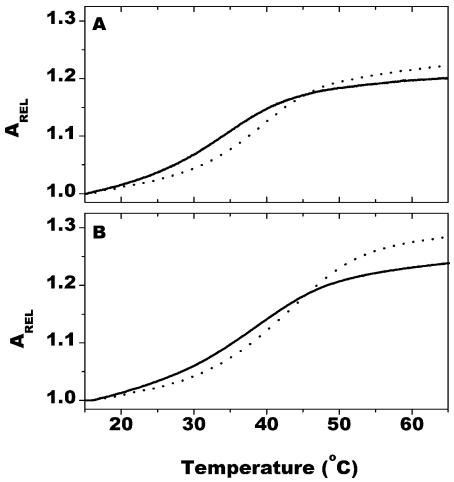

FIGURE 2: Relative absorbance vs temperature curves of DNA UV melting profiles of duplex $(AA)_2AGCT(TT)_2$ (dotted curves) and $(AT)_2AGCT(TA)_2$ (solid curves) in BPES buffer. (A) DNA alone. (B) 1:1 ratio of 7-amino ACTD with DNA; DNA duplex was prepared as described in the Materials and Methods.

DNA Stability and their Structure. Figure 2A shows typical optical melting curves obtained for the DNA molecules shown in Figure 1. Specifically, the 12-mer $(AT)_2$ and $(AA)_2$ duplex DNA molecules are depicted. The nearly identical shapes of the melting transitions suggest that end-fraying is not a problem. It is apparent that the DNA molecule containing the $(AA)_2$ flanking sequence (dotted curve) is more stable than the one containing $(AT)_2$ (solid curve). The difference in T_m of the two duplexes is 5.5 °C. This is in good agreement with the predictions using published nearest neighbor parameters (*34*). Both sequences also display comparable hyperchromicity changes upon melting (not shown), approximately 20%.

Table 1 summarizes the melting data collected for the seven DNA molecules. For the same length $(AA)_n$ and $(AT)_n$ series, the $(AA)_n$ flanks are more stable than the $(AT)_n$ flanks. Interestingly, the stability of the $(AA)(AT)_2$ hybrid DNA molecule is intermediate between the stability of the $(AT)_3$ and $(AA)_3$ molecules.

CD spectra for the DNA molecules are shown in Figure 3. Figure 3A,B shows the CD spectra of these seven DNA molecules alone. The recorded CD spectra are essentially B-form. Molar ellipticity increases with increasing length of the flanking sequence. However, subtle spectroscopic differences exist for the $(AT)_n$ and $(AA)_n$ series DNA molecules. For the $(AT)_n$ DNA molecules (Figure 3A), the maximum positive band was at about 273 nm. This band shifted to 278 nm for the $(AA)_n$ fragments (Figure 3B), and the hybrid $(AA)(AT)_2$-DNA spectra was essentially the same as the $(AT)_n$ molecules, consistent with its comparatively lower stability as compared to the $(AA)_3$ molecule. From UV melting data and CD experiments, it can be seen that

Table 1: Summary of DNA Stability and Their Binding Affinity to 7-AminoACTD in BPES Buffer[a]

DNA	T_m^0 (°C)	T_m (°C)	ΔT (°C)	K (M duplex)$^{-1}$	N (duplex)	$R = F_b/F_0$	τ (ns)
$(AT)_2$	35.0	39.0	4.0	3.73×10^5	1.0	8.34	0.511 < 0.487, 0.535 >
$(AT)_3$	42.5	45.0	2.5	2.52×10^5	1.0	8.41	0.519 < 0.493, 0.544 >
$(AT)_4$	51.0	52.5	1.5	2.32×10^5	1.1	9.40	0.537 < 0.516, 0.558 >
$(AA)(AT)_2$	45.5	48.0	2.5	1.81×10^5	1.2	8.60	0.527 < 0.504, 0.550 >
$(AA)_2$	40.5	44.5	4.0	1.15×10^5	1.1	8.40	0.517 < 0.490, 0.544 >
$(AA)_3$	49.0	51.5	2.5	9.98×10^4	1.2	7.80	0.508 < 0.484, 0.532 >
$(AA)_4$	54.5	56.0	1.5	9.62×10^4	1.1	7.10	0.486 < 0.468, 0.504 >

[a] $\Delta T = T_m - T_m^0$; T_m and T_m^0 refer to the melting temperature of DNA in the presence or absence of 7-amino ACTD (1:1) in BPES buffer, respectively. The estimated error for the T_m values was less than 0.5 °C. N was their binding stoichiometry. R and τ values were obtained from steady-state fluorescence and lifetime measurements at the same binding ratio (r = [ligand]/[DNA] =1:100(strand)).

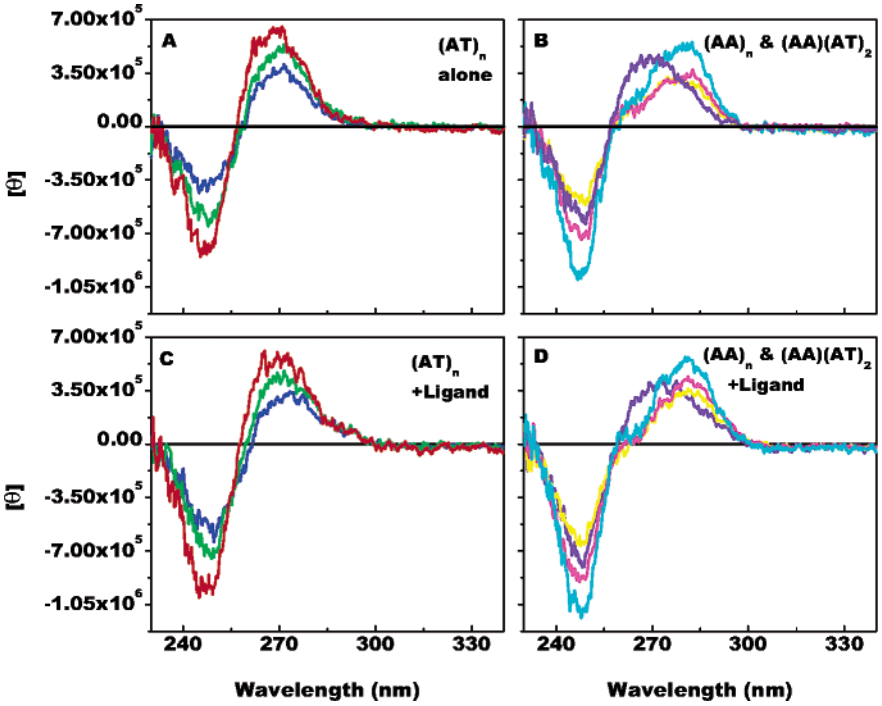

FIGURE 3: Circular dichroism spectra of these seven duplex DNA molecules in BPES buffer. (A) $(AT)_n$-series DNA alone; (B) $(AA)_n$-series DNA and $(AA)(AT)_2$-DNA alone; (C) 1:1 ratio of 7-amino ACTD with $(AT)_n$-series DNA; and (D) 1:1 ratio of 7-amino ACTD with $(AA)_n$-series DNA and $(AA)(AT)_2$-DNA. $(AT)_2$-, $(AT)_3$-, and $(AT)_4$-DNA are shown as red, green, and blue lines, respectively; $(AA)_2$-, $(AA)_3$-, $(AA)_4$-, and $(AA)(AT)_2$-DNA are shown as cyan, magenta, yellow, and violet lines, respectively.

the different flanking sequence contexts affect total DNA stability and their secondary structures.

DNA Flanking Sequence and Fluorescence Enhancement of 7-Amino ACTD. When 7-amino ACTD bound to the seven DNA duplex molecules, its fluorescence was greatly enhanced (see Supporting Information). More importantly, enhancement of the fluorescence intensity or the fluorescence lifetime of 7-amino ACTD at the same binding ratio (r = [ligand]/[DNA]) varies depending on the flanking sequence context. Results of fluorescence measurements are summarized in Table 1. For 7-amino ACTD bound to the $(AT)_n$ series, both the intensity ratio of bound to free (F_b/F_0) species and their lifetime, τ, increased with increasing flanking sequence length (n = 2, 3, 4). This is consistent with the trend observed for the DNA thermodynamic stability. However, the opposite behavior was found for the ratio of F_b/F_0 and τ for the $(AA)_n$ flanking sequences context. The trend in fluorescence enhancements with flanking sequence length was opposite to the DNA stability. That is, the fluorescence enhancements decreased with increased length. Previous DNase I footprinting and imino proton NMR studies asserted that context effects are more transmittable in $d(AT)_3$ sequences than that in $d(AA)_3$ sequences (*35*). If fluorescence enhancements correspond to transmittability, our results are consistent with the published observations. However, differences in the thermodynamic or spectroscopic properties of the $(AT)_n$ and $(AA)_n$ sequences were not reported in that study. Since the excited state of the fluorophor is sensitive to the microenvironment provided by the different DNA flanking sequences, fluorescence enhancements provide the assessment of subtle differences in DNA sequences. However, such enhancements are not able to provide evaluations of ligand binding affinity.

Ligand Binding Affinity and DNA Flanking Sequence. A fluorescence-based assay was employed to measure the binding affinity of 7-amino ACTD for each member of the set of seven DNA molecules depicted in Figure 1. Figure 4 shows typical binding isotherms obtained by titering 7-amino ACTD into solutions of the $(AT)_2$ and $(AA)_2$ DNA isomers. Nonlinear least-squares analysis of the fluorescence titration curves yielded ligand binding constants of 3.73×10^5 (M duplex)$^{-1}$ and 1.15×10^5 (M duplex)$^{-1}$ for the $(AT)_2$ and

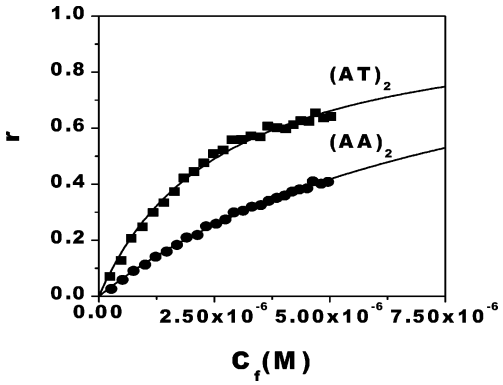

FIGURE 4: Representative binding isotherms for the interaction of 7-amino ACTD with the DNA duplexes. Shown here are the isotherms for $(AT)_2$ DNA (square points) and $(AA)_2$ DNA (circle points). The solid lines are nonlinear least squares regression fits to the data. The binding model applied to analyze and evaluate the binding constants was described in the Materials and Methods. Values of the binding constants are summarized in Table 1.

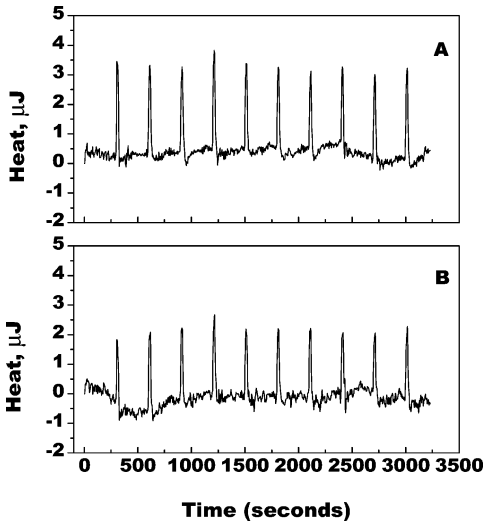

FIGURE 5: Comparison of ITC studies of 7-amino ACTD titrated into the DNA duplexes in BPES buffer at 20 °C. Panel A: $(AT)_2$-DNA and panel B: $(AA)_2$-DNA. Each peak shows the heat produced by a serial injection of an aliquot of dye solution (3 μL of 0.3 mM) into the DNA solution (1.13 mL of 100 μM in strand).

$(AA)_2$ duplex, respectively. Thus, the ligand binding affinity is significantly enhanced when the primary site is flanked by an $(AT)_2$ sequence that is less stable, but stability increases after ligand intercalation. Titration data were fit directly by nonlinear least-squares methods. Errors in the binding parameters resulting from the fitting procedure were within 10%, carefully evaluated by Monte Carlo analysis (*27*). Differences in binding affinity between the other $(AT)_n$ versus $(AA)_n$ series DNA molecules were also observed. These results are summarized in Table 1. Binding affinity ratios for different flanking sequences of the same length, $K_{(AT)n}/K_{(AA)n}$, are 3.24, 2.53, and 2.40 (n = 2, 3, 4), respectively. Within experimental error, the 7-amino ACTD binding stoichiometry was 1:1 for all DNA molecules. This is in good agreement with a previous study employing DNA molecules containing a single binding site (-A-G-C-T-) (*22*). Comparison of the measured stability with the observed binding affinity of the ligand for the set of DNA molecules reveals an inverse relationship. The binding affinity decreased with increasing flanking sequence length irrespective of the sequence context. Our melting results are consistent with previous findings and confirm previous observations.

As shown by the ΔT_m values in Table 1, melting temperatures of the DNAs increase when 7-amino ACTD is bound to the $(AT)_n$ and $(AA)_n$ DNA molecules. Typical optical melting curves for DNA/ligand mixtures are displayed for the $(AT)_2$ and $(AA)_2$ isomers in Figure 2B. For the $(AT)_2$ or the $(AA)_2$ fragment, the difference in T_m for DNA with ligand bound and DNA alone ($\Delta T = T_m - T_m^0$) was about 4 °C. At the same [ligand]/[DNA] ratio, the ΔT decreased with increasing length (see Table 1), inferring that the binding affinity declines with longer flanking sequences. This is in good agreement with the fluorescence binding studies. It should be noted that this trend may not be completely general.

CD measurements indicate that the DNA molecules adopt a typical B-type structure and that ligand binding does not appear to significantly alter DNA secondary structure (Figure 3C,D). This implies that 7-amino ACTD does not dramatically alter DNA secondary structure when it intercalates at its primary binding site. Still, subtle structural differences exist for the DNA molecules. These differences can only be attributable to the different flanking sequences and must also affect DNA stability and binding affinity. All these results taken together suggest that the 7-amino ACTD binding affinity for DNA is modulated by flanking sequence stability. In addition, these effects do not appear to be due to permanent changes in DNA secondary structure associated with ligand binding.

Thermodynamic Parameters of Ligand/DNA Interactions. The enthalpy change associated with the formation of a 7-amino ACTD/duplex DNA complex was measured directly utilizing isothermal titration calorimetry (ITC). Typical data for 7-amino ACTD adding to solutions of $(AT)_2$ and $(AA)_2$ DNA are shown in Figure 5. The binding enthalpy, ΔH_{bind}, for each reaction was obtained from at least three separate experiments. The data are summarized in Table 2. By directly measuring the enthalpy change associated with DNA/ligand complex formation, reliable comparisons of the thermodynamic parameters for DNA/ligand interactions can be made.

Figure 6 shows the relationships between the thermodynamic parameters of binding for the different DNAs. It appears that 7-amino ACTD binding to these seven DNA molecules is enthalpy-driven, along with favorable entropy contributions. For example, the enthalpy was −6.80 and −5.26 kcal/mol for 7-amino ACTD binding to $(AT)_2$- and $(AA)_2$-DNA, respectively. Interestingly, the favorable entropy change was 2.29 cal/deg mol for $(AT)_2$ and 5.19 cal/deg mol for $(AA)_2$, indicating that the entropy contribution modulated the DNA/ligand interaction by compensating for their apparent binding enthalpy differences. Similar binding thermodynamic characteristics were also observed for 7-amino ACTD binding to the other DNAs.

A plot of the values of $-\Delta H_{bind}$ versus ΔS_{bind} (taken from Table 2) is shown in Figure 7A. A least-squares linear regression fit of the points (correlation coefficient, $R > 0.97$) demonstrates the linear relationship between the enthalpies and the entropies of 7-amino ACTD binding. As this plot indicates, the binding entropy decreases when the binding enthalpy increases. One explanation for this observation is that as the ligand forms favorable interactions in the primary

Table 2: Thermodynamic Parameters of DNA Alone and for Binding of 7-Amino ACTD

DNA	$-\Delta H_{DNA}$[a] (kcal/mol)	$-\Delta H_{bind}$[b] (kcal/mol)	$-\Delta S_{DNA}$[a] (cal/deg mol)	ΔS_{bind}[b] (cal/deg mol)	$-\Delta G_{DNA}$[a] (kcal/mol)	$-\Delta G_{bind}$[c] (kcal/mol)
$(AT)_2$	63.0	6.80	190	2.29	6.2	7.47
$(AA)_2$	56.5	5.26	168	5.19	6.5	6.78
$(AT)_3$	75.0	7.01	225	0.78	7.9	7.24
$(AA)_3$	78.0	5.66	230	3.55	9.5	6.70
$(AA)(AT)_2$	75.7	5.84	226	4.13	8.3	7.05
$(AT)_4$	123.5	6.45	370	2.53	13.2	7.19
$(AA)_4$	136.2	4.85	404	6.25	15.8	6.68

[a] DNA data taken from Benight et al. (*34*). [b] Binding enthalpy determined directly by ITC and used to calculate the entropy change, using $\Delta G° = \Delta H° - T\Delta S°$. [c] Net binding free energy calculated using $\Delta G_{bind} = -RT \ln K$. Binding constant K determined from fluorescence titrations in BPES buffer (pH 7.0) at 20 °C and summarized in Table 1.

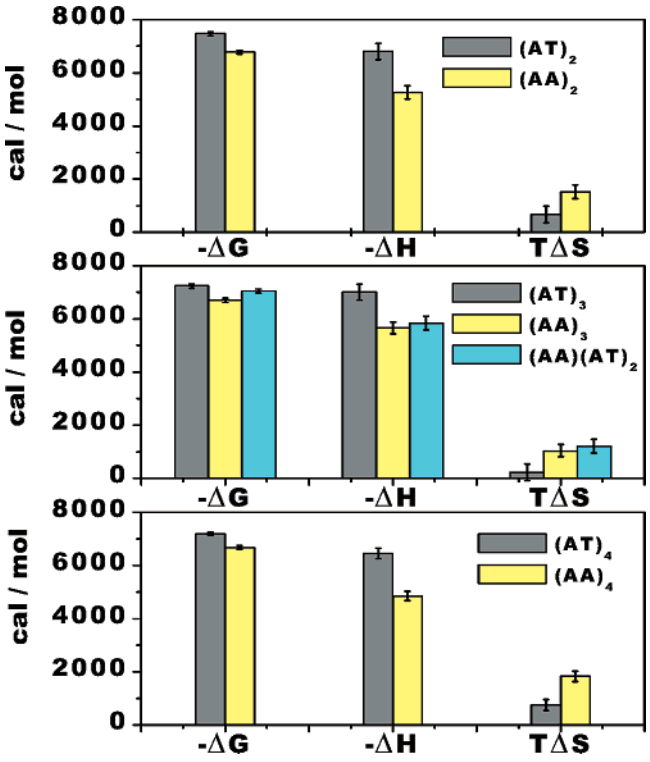

FIGURE 6: Comparison of the enthalpic and entropic contributions to the binding free energy of 7-amino ACTD bound to the DNA isomers. $(AT)_2$ and $(AA)_2$: upper panel; $(AT)_3$, $(AA)_3$, and $(AA)(AT)_2$: middle panel; and $(AT)_4$ and $(AA)_4$: bottom panel, at 20 °C, where $\Delta G_{bind} = \Delta H_{bind} - T\Delta S_{bind}$.

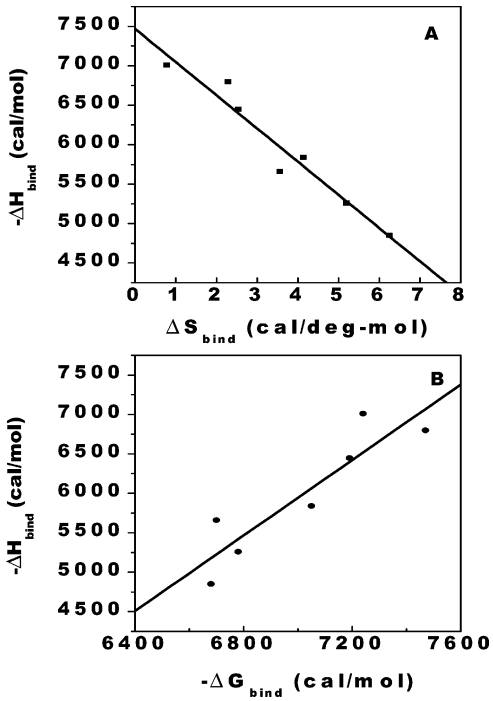

FIGURE 7: Relationship between the enthalpy and the entropy of 7-amino ACTD binding to the seven DNA molecules. Panel A: plot of $-\Delta H_{bind}$ vs ΔS_{bind} and panel B: plot of $-\Delta H_{bind}$ vs $-\Delta G_{bind}$. The two solid lines through the data were the best fit curves. Values plotted were taken from Table 2.

binding site via base pair intercalation, solvent molecules associated with the hydration shell of the ligand molecule and residing in the binding pocket in the minor groove and intercalation site of the DNA become rearranged. This is a classic example of enthalpy/entropy compensation occurring to produce a favorable ligand/substrate complex (*36*, *37*). The constant value of the slope of the plot in Figure 7A, referred to as the compensation temperature (*36*), T_c, was 420 ± 46 K. This was close to the reported value of 400 ± 30 K evaluated in studies of the ionic strength dependence of binding cytosine 3′-phosphate (3′-CMP) to RNase A (*36*) but much higher than our experimental reaction temperature of 293 K. Similarly, a plot of $-\Delta H_{bind}$ versus $-\Delta G_{bind}$ (shown in Figure 7B) is also linear ($R > 0.91$), again a characteristic of classical enthalpy/entropy compensation (*37*).

Enthalpy/entropy compensation has been widely observed and reported for the binding of ligands to proteins (*36*−*38*). For protein−ligand interactions, explanations of the molecular basis of the enthalpy/entropy compensation have focused on the involvement of water molecules rearranged in the binding processes (*36*−*38*). Different fluorescence enhancements of 7-amino ACTD when bound to different DNA sequences (Table 1), and the observed compensation between the binding enthalpy change, ΔH_{bind}, and the binding entropy change, ΔS_{bind}, might be due to differences in the flanking sequence ($(AT)_n$ or $(AA)_n$) surrounding the primary binding site, which consists of central base pairs, AGCT. Recent studies have shown that at least two hydration layers surround duplex DNA and that the ordering of the layers of DNA hydration is sequence dependent (*39*, *40*). Highly ordered water molecules in the hydration layers have also been observed in high-resolution structures of DNA oligomers bound to ligands such as actinomycin D (a derivative of the antitumor drug studied here) and daunomycin (*15*, *22*), and this property is not restricted to intercalating ligands. Hydration layers are also evident from the high-resolution crystal structures of minor groove binders, such as berenil or bis(amidine) ligands and from related NMR studies (*41*−*44*). Ordered waters clearly have an important effect upon

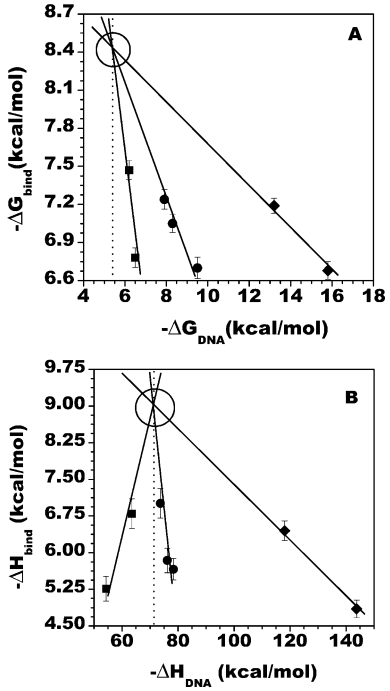

FIGURE 8: Panel A: Correlation between the free energy of ligand binding ($-\Delta G_{bind}$) and free energy of melting ($-\Delta G_{DNA}$). Isomers of $(AT)_2$ and $(AA)_2$: square symbols; $(AT)_3$, $(AA)(AT)_2$, and $(AA)_3$: circle symbols; and $(AT)_4$ and $(AA)_4$: diamond symbols. The interception point is $\Delta G_{DNA} = -5.30$ kcal/mol. Panel B: binding enthalpy change ($-\Delta H_{bind}$) vs the enthalpy change of DNA duplex melting ($-\Delta H_{DNA}$). Symbol designations are the same as those used in panel A to represent the DNA molecules.

ligand binding. Therefore, as discussed previously (*2*), when these intercalating ligands bind to DNA, base pairs are separated, and the DNA is locally unwound to accommodate the ligand. This results in a kind of local stretching of the phosphate backbone that alters and reduces some degrees of freedom at the intercalation site (*2*). The latter change also reduces the local charge density and would necessarily result in the release of condensed counterions (*2*, *4*). Many important direct and indirect interactions would take place between the ligand, DNA, and surrounding solvents; formation of specific hydrogen bonds between the ligand and DNA was possibly mediated by water molecules (*15*, *22*). Water layer rearrangement along the minor groove at the binding site, complex specific van der Waals interactions, electrostatic interactions, and a variety of new and reorientated stacking interactions could occur in the formation of the intercalation complex. Upon intercalation, different DNA duplex molecules with $(AT)_n$ or $(AA)_n$ flanking sequences could respond to these changes in different ways with effects translating beyond the primary binding site (*27*). Thus, different flanking sequences could make different contributions to the indirect interactions involved in 7-amino ACTD/DNA complex formation. This could also be mediated by water and other solvent molecules (*2*, *15*, *22*). Since all the DNA molecules studied here have the same intrinsic binding site, 5′-A-G-C-T-3′, the flanking sequences must give rise to the observed enthalpy/entropy compensation.

Comparison of the Binding and Melting Free Energies. Figure 8A shows the relationship between the binding free energies, ΔG_{bind}, and the DNA melting free energies, ΔG_{DNA} (taken from Table 2). Clearly, small changes in DNA stability result in relatively large enhancements of ligand binding, indicating that flanking sequence stability has a strong effect on the binding of 7-amino ACTD to its primary binding site. Apparently, the relationship between the binding free energy (ΔG_{bind}) for 7-amino ACTD bound to a particular length duplex DNA, and the melting free energy of the DNA duplex (ΔG_{DNA}) is linear. Extrapolation of the fitted lines in Figure 8A results in a common intersection point. A similar intersection point with a melting free energy of -5.20 kcal/mol was found in binding studies of AluI restriction enzyme to the same set of DNA molecules (*34*). The intersection point was taken to correspond to the binding free energy (ΔG_{bind}) of the ligand bound to the four base pair core sequence AGCT alone, with a melting free energy of -5.30 kcal/mol, in precise agreement with the melting free energy of the four base pair sequence, AGCT, calculated using the $n-n$ sequence dependent parameters (*34*).

A plot of the binding enthalpy, ΔH_{bind}, versus the melting enthalpy, ΔH_{DNA}, is shown in Figure 8B. Again after extrapolation, a common intersection point is obtained, further supporting the notion that the binding site comprised of the core tetramer sequence AGCT only maintains the same intrinsic binding characteristics of the other sequences and that the flanking sequence apparently modulates the binding of 7-amino ACTD to the primary binding site.

Using values corresponding to the intersection points in Figure 8A, the intrinsic binding entropy of the core sequence can be calculated by the equation $\Delta S_{bind}(0) = (\Delta H_{bind}(0) - \Delta G_{bind}(0))/T$. At $T = 293$ K, $\Delta S_{bind}(0)$ is -2.01 cal/deg mol, which implies that 7-amino ACTD binding to the core sequence, AGCT, is entirely enthalpically driven and entropically unfavorable. In contrast, as shown in Figure 6, a favorable entropy contribution is observed for 7-amino ACTD binding to the entire duplex DNA having the common central four base sequence 5′-A-G-C-T-3′ flanked on either side by the sequences $(AT)_n$ or $(AA)_n$. Thus, flanking sequences surrounding the primary binding site affect the entire binding process and result in a net favorable compensation between the binding enthalpy change, ΔH_{bind}, and the binding entropy change, ΔS_{bind}, associated with the ligand DNA interaction.

In summary, subtle DNA structural differences can be detected by fluorescence techniques. Different flanking sequence contexts of A·T and T·A base pairs surrounding the central base sequence (AGCT) lead to different enhancements of ligand fluorescence intensities and lifetimes. For the $(AA)_n$ flanking sequence, fluorescence enhancement declined with increasing flanking sequence length, opposite from the trend in fluorescence enhancement observed for $(AT)_n$ flanking sequences. Our studies clearly show that the binding of 7-amino ACTD to its core sequence in these seven short DNA oligomers is strongly affected by differences in length and context of the flanking sequence, and binding affinity is inversely proportional to flanking sequence stability. Enthalpy−entropy compensation was found accompanying the favorable interaction between ligand and DNA.

ACKNOWLEDGMENT

The authors are grateful for the referees' helpful comments on the manuscript.

SUPPORTING INFORMATION AVAILABLE

Two figures of primary emission and excition spectra. This material is available free of charge via the Internet at http://pubs.acs.org.

REFERENCES

1. Wade, W. S., Mrksich, M., and Dervan, P. B. (1992) *J. Am. Chem. Soc. 118*, 8783−8794.
2. Chaires, J. B. (1997) *Biopolymers 44*, 201−215.
3. Laughton, C. A., Tanious, F., Nunn, C. M., Boykin, D. W., Wilson, W. D., and Neidle, S. (1996) *Biochemistry 35*, 5655−5661.
4. Bailly, C., Qu, X., Graves, D. E., Prudhomme, M., and Chaires, J. B. (1999) *Chem. Biol. 6*, 277−286.
5. Chaires, J. B. (1996) *Anticancer Drug Des. 11*, 569−580.
6. Hopkins, H. P., Jr., and Wilson, W. D. (1987) *Biopolymers 26*, 1347−1355.
7. Bailly, C., Qu, X., Anizon, F., Prudhomme, M., Riou, J., and Chaires, J. B. (1999) *Mol. Pharmacol. 55*, 377−385.
8. Crothers, D. M. (1971) *Biopolymers 10*, 2147−2160.
9. Chou, W. Y., Marky, L. A., Zaunczkowski, D., and Breslauer, K. (1987) *J. Biomol. Struct. Dyn. 5*, 345−359.
10. Ren, J., and Chaires, J. B. (1999) *Biochemistry 38*, 16067−16075.
11. Chaires, J. B., Dattagupta, N., and Crothers, D. M. (1982) *Biochemistry 21*, 3933−3940.
12. Chen, F.-M. (1988) *Biochemistry 27*, 6393−6397.
13. Bailey, S. A., Graves, D. E., and Rill, R. (1994) *Biochemistry 33*, 11493−11500.
14. Hardenbol, P., Wang, J. C., and Van Dyke, M. W. (1997) *Bioconjugate Chem. 8*, 617−620.
15. Frederick, C. A., Williams, L. D., Ughetto, G., van der Marel, G. A., van Boom, J. H., Rich, A., and Wang, A. H.-J. (1990) *Biochemistry 29*, 2538−2549.
16. Pelaez, R., de Clairac, L., Geierstanger, B. H., Mrksich, M., Dervan, P. B., and Wemmer, D. E. (1997) *J. Am. Chem. Soc. 119*, 7909−7916.
17. Chaires, J. B., Fox, K. R., Herrera, J. E., Britt, M., and Waring, M. J. (1987) *Biochemistry 26*, 8227−8236.
18. Blakesly, R. W. (1987) in *Gene Amplification and Analysis* (Chirikjian, J. G., Ed.) pp 51−102, Elsevier Science, New York.
19. Riccelli, P. V., Vallone, P. M., Kashin, I., Faldasz, B. D., Lane, M. J., and Benight, A. S. (1999) *Biochemistry 38*, 11197−11208.
20. Vallone, P. M., and Benight, A. S. (2000) *Biochemistry 39*, 7835−7846.
21. Chen, F.-M. (1998) *Biochemistry 37*, 3955−3964.
22. Kamitori, S., and Takusagawa, F. (1992) *J. Mol. Biol. 225*, 445−456.
23. Amaratunga, M., Pancoska, P., Paner, T. M., and Benight, A. S. (1990) *Nucleic Acids Res. 18*, 577−582.
24. Paner, T. M., Amaratunga, M., Doktycz, M. J., and Benight, A. S. (1990) *Biopolymers 29*, 1715−1734.
25. Fasman, G. D. (1975) *CRC Handbook of Biochemistry and Molecular Biology*, 3rd ed., Vol. I, pp 589, CRC Press, Cleveland, OH.
26. Ren, J., Qu, X., Chaires, J. B., Trempe, J. P., Dignam, S. S., and Dignam, J. D. (1999) *Nucleic Acids Res. 27*, 1985−1990.
27. Qu, X., Trent, J. O., Fokt, I., Priebe, W., and Chaires, J. B. (2000) *Proc. Natl. Acad. Sci. U.S.A. 96*, 12032−12037.
28. Haq, I., Ladbury, J. E., Chowdhry, B. Z., Jenkins, T. C., and Chaires, J. B. (1997) *J. Mol. Biol. 271*, 244−257.
29. *29.* Ren, J., Jenkins, T. C., and Chaires, J. B. *Biochemistry 39*, 8439−8447.
30. Wadkins, R. M., and Jovin, T. M. (1991) *Biochemistry 30*, 9469−9478.
31. Bailey, S. A., Graves, D. E., Rill, R., and Marsch, G. (1993) *Biochemistry 32*, 5881−5887.
32. Takusagawa, F., Wen, L., Chu, W. H., Li, Q. F., Takusagawa, K. T., Carlson, R. G., and Weaver, R. F. (1996) *Biochemistry 35*, 13240−13249.
33. Yung, B. Y. M., Chang, F. J., and Bor, A. M. S. (1991) *Cancer Lett. 60*, 221−227.
34. Benight, A. S., Gallo, F. J., Paner, T. M., Bishop, K. D., Faldasz, B. D., and Lane, M. J. (1995) *Advances in Biophysical Chemistry*, Vol. 5, pp 1−55, JAI Press Inc., Greenwich, CT.
35. Bishop, K. D., Borer, P. N., Huang, Y.-Q., and Lane, M. J. (1991) *Nucleic Acids Res. 19*, 871−875.
36. Eftink, M. R., Anusiem, A. C., and Biltonen, R. L. (1983) *Biochemistry 22*, 3884−3896.
37. Lumry, R., and Rajender, S. (1970) *Biopolymers 9*, 1125−1227.
38. Sturtevant, J. (1977) *Proc. Natl. Acad. Sci. U.S.A. 74*, 2236−3699.
39. Berman, H. M. (1994) *Curr. Opin. Struct. Biol. 4*, 345−350.
40. Shui, X., McFail-Isom, L., Hu, G. G., and Williams, L. D. (1998) *Biochemistry 37*, 8341−8355.
41. *41.* Brown, D. G., Sanderson, M. R., Skelly, J. V., Jenkins, T. C., Brown, T., Garman, E., Stuart, D. I., and Neidle S. (1990) *EMBO J. 9*, 1329−1334.
42. *42.* Edwards, K. J., Jenkins, T. C., and Neidle, S. (1992) *Biochemistry 31*, 7104−7109.
43. *43.* Nunn, C. M., Jenkins T. C., and Neidle, S. (1993) *Biochemistry 32*, 13838−13843.
44. *44.* Lane, A. N., Jenkins, T. C., and Frenkiel, T. A. (1997) *Biochim. Biophys. Acta 1350*, 205−220.

BI0347813